Development of a Ti-based Alloy: Design and Experiment

Haitham El Kadiri, Liang Wang, H. Ozkan Gulsoy, Pavan Suri, Seong Jin Park, Youssef Hammi, and Randall M. German

We proposed the design methodology for titanium-based alloys based on a combination of literature survey, simulation, and experiment. We have selected and investigated the properties of novel Ti-Fe-Zr alloys specifically designed for densification via powder metallurgy techniques. Samples were produced by die compaction of mixed elemental powders with subsequent densification by sintering at 1,275°C in vacuum. Scanning electron microscopy and optical microscopy were used to examine the sintered microstructures to compliment hardness and tensile testing. The results show that density and mechanical properties increase with the iron and zirconium content. The best property combination was obtained with the addition of 5 wt.% iron and 5 wt.% zirconium when vacuum sintered at 1,275°C for 60 min.

INTRODUCTION

The high strength-to-density ratio and excellent corrosion resistance of titanium alloys make them the subject of numerous studies for the development of cost-effective alloys.[1] The high cost is evident in all aspects of such alloys, such as in the extraction of raw materials, exotic alloying elements, metalworking cycles, and machining difficulty.[2] In our work targeted toward low-cost automotive application, attention is given to titanium powder metallurgy (PM) for cost reduction via the production of net-shape components.[3] As a net-shape process, PM can minimize machining and be noticeably versatile in terms of microstructure design through alloying and sintering. Improvements in net-shaping technology coupled with the availability of low-cost powders will increase the usage of titanium alloys and enable product designs that effectively utilize the alloys.[4–6] Successful PM titanium products first emerged using hot isostatic press (HIP) technology. Elimination of porosity, critical to achieve acceptable mechanical properties, has proven challenging in conventional pressure-less sintering techniques. For this reason, HIP products still constitute the major commercialized PM titanium components in modern aircraft and automotive industries.[7,8] Hot isostatic pressing is too expensive for the large-scale production of PM titanium components.

In this work we assume a pragmatic improvement might be possible using a powder metallurgy process and returning to the powder chemo-mechanical design level.[9] Over the last decade, instead of using prealloyed (PA) powder, hydrogenated blended elemental (BE) titanium powder has proven an effective means to improve the sintered density.[9] Hydrogen embrittlement of the powder promotes crushability into small particles useful for sintering densification. However, to date the sintered density is still ineffective in delivering a high tensile ductility and high fatigue resistance.

Near full density can be achieved via vacuum sintering of titanium alloys with an appropriate choice of particle size, purity, and powder mixtures to alloy during sintering. Improvements in sintered density and mechanical properties are possible using prealloyed powders and blended elemental powders obtained via a hydride-dehydride process.[9] Small powders obtained by crushing titanium hydride have the low oxygen content and sintering potential to eliminate porosity at sintering temperatures similar to those used for stainless steels.

Accordingly, several titanium alloys have been developed over the years, including variants that contain Fe, Zr, Al, V, Mo, and Ta as major alloying elements. Example alloys include Ti-5Al-2Cr-1Fe, Ti-6.8Mo-4.2Fe-1.4Al-1.4V, Ti-4.5Al-3V-2Fe-2Mo, Ti-8Fe-8Ta-4Zr, Ti-10Fe-10Ta-4Zr.[6] Along the way alloying with copper was investigated due to its ability to form a transient liquid phase, but little has been published on this approach. Many of the current alloys are expensive due to the alloying additions. To lower material cost and improve properties, iron is an attractive alloying element.[10,11] In turn, zirconium is suitable for increasing strength.[12] The combination of iron and zirconium is

How would you…

…describe the overall significance of this paper?

This paper offers a methodology of developing cost-effective titanium alloys via a powder metallurgy technique. It presents the overall barriers in the literature and suggests a technical road map to design a titanium-based alloy that may offer good strength and a more affordable price.

…describe this work to a materials science and engineering professional with no experience in your technical specialty?

This work was initiated under the concern that contemporary titanium alloys can not be made with good strength without a substantial increase in cost. The reasons stem from a fundamental premise. This work tries to suggest a methodology rather than an ultimate solution.

…describe this work to a layperson?

Modern aircraft and automotive engines need to be lightweighted under the modern and future constraints of an oil economy. Titanium alloys are excellent lightweight materials candidates for both applications. This work attempts to overcome current barriers to commercializing titanium alloys.

one means to promote a high sintered density and good properties via liquid phase sintering. Further property gains should be possible by post-sintering heat treatment.

In this study, the effect of various compositions of a Ti-Fe-Zr system are examined with respect to chemical homogenization and pore closure during vacuum sintering over a range of sintering temperatures and times. Liquid phase sintering is employed, where the iron and zirconium promote densification and improve sintered strength. Further, the ability to form the β phase opens the possibility of heat treatment during cooling or after sintering to further enhance mechanical properties. Thermo-Calc software was used to predict phase diagrams and compute composition modulation profiles from elemental powders. These simulation techniques were used to rationalize microstructures observed through scanning electron microscopy (SEM) and optical microscopy. This study does not propose a novel alloy, but provides important insights into the mutual effect of iron and zirconium on chemical homogenization, pore closure, and β-grain refinement.

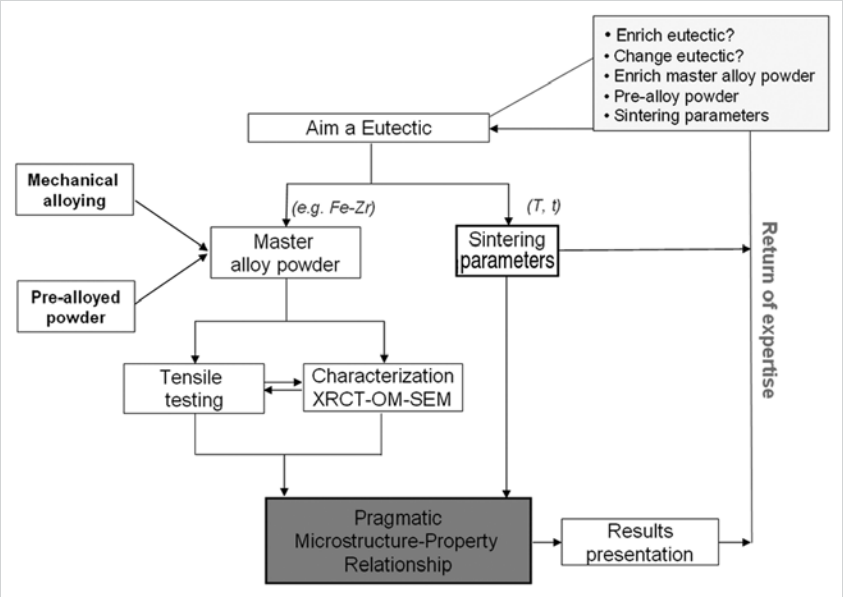

Figure 2. A composition optimization algorithm for liquid phase sintering of titanium alloy powder.

TITANIUM ALLOY DESIGN

Titanium alloys can be a predominantly monophase structure: α (hexagonal close-packed, hcp) or β (body-centered cubic, bcc), or a dual phase structure α + β, depending on the ratio between the α-stabilizing and β-stabilizing elements. Figure 1 schematically illustrates the main properties of potential titanium alloys falling in different crystallographic classes.[1] α alloys only enclose traces of β phase. Near-α alloys contain predominantly α phase and the microstructure may appear similar to an α alloy. A dual-phase α-β alloy consists of α and retained or partially transformed β. Metastable β alloys predominantly retain β phase, which is susceptible to a fine transformation upon heat treatments.

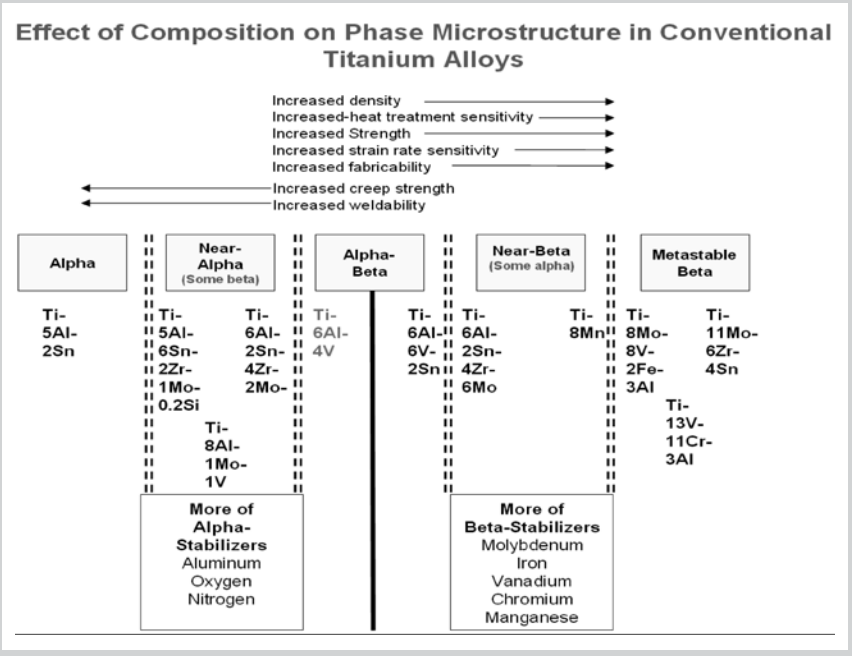

Figure 1. The general classification of titanium alloys with respect to properties and microstructure.[1]

For suitable mechanical properties, metastable β is needed to a certain extent to improve hardenability.[13] In fact, for titanium alloys, if creep resistance is not the only concern, strength is primarily related to the balance between the extent of "displacively" transformed β products (martensite α′, martensite α″, Widmanstätten ferrite α_w), the coarseness or fineness of retained β, and the size and shape of prior β grains. This calls for the need of both α-stabilizers and β-stabilizers. The main compositions that found wide interest were based on Ti-xAl-yV and Ti-xAl-yFe systems,[11,14] where aluminum is a strong α-stabilizer and vanadium and iron are β stabilizers.[1] The second system was a cost-conscious design.

Nonetheless, these near α/dual-phase α titanium systems could not be hot isostatically pressed to full density without a noticeable impairment in the mechanical properties. Chemical homogenization was one of the main impediments. Elemental aluminum melts and diffuses into titanium at relatively low temperatures, forming an α-layer around the prior particle boundaries of titanium. This layer acts as a diffusion barrier for vanadium or iron resulting in an inhomogeneous microstructure. Residual pore

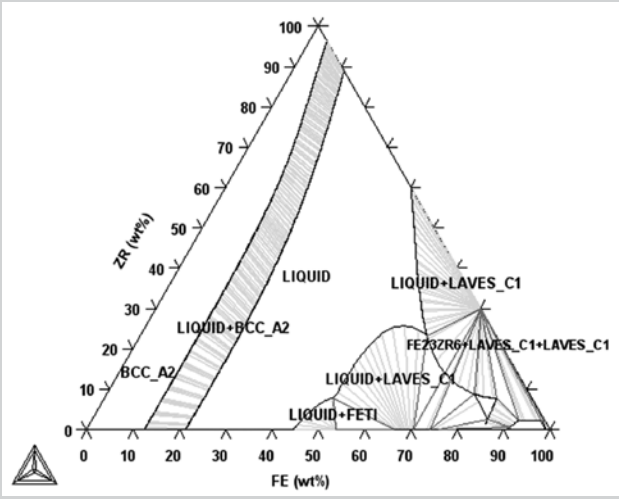

Figure 3. A Ti-Fe-Zr ternary phase diagram calculated by Thermo-Calc at a sintering temperature of 1,275°C.

formation due to the solubility of alloying elements, especially aluminum, is another mitigating factor.[11] The amount of alloy addition is limited by the formation of intermetallics. In a binary Ti-Fe alloy, iron content in excess of 3 wt.% results in the formation of brittle FeTi intermetallic precipitate along the titanium prior particle boundary. Other investigations include the use of elemental powders in combination with refractory precipitates or TiC and TiB precipitates via in situ reactions to limit grain and β-phase coarsening during sintering. The success of most of these approaches in obtaining near full dense products with good balance of strength and ductility is relatively muted.[15–18]

Zirconium is a good substitute for aluminum as an alloying element. Zirconium stabilizes the α and β phases and promotes chemical homogenization. Its affinity toward oxygen and carbon, solubility in titanium and eutectic with iron at 928°C are a few characteristics that are favorable for densification and chemical homogenization. Although more costly than aluminum, zirconium is less expensive than vanadium by almost six orders of magnitude. Further, zirconium provides good creep resistance and stabilizes silicate particles when needed.

Based on our literature survey and research, we recommend to start with the following three compositions using master allow powder for generating the eutectic systems:

- Alloy 1: Ti–(1-3)Fe–(1-3)Mo–(2-6)Zr–(1-4)Sn–(1-2)Cr
- Alloy 2: Ti–(1-3)Fe–(1-3)Mo–(2-6)Zr–(1-4)Sn–(1-3)Mn–(1-2)Cr
- Alloy 3: Ti–(1-3)Fe–(1-3)Mo–(2-6)Zr–(1-4)Sn–(1-3)Mn–(1-5)Cr_3C_2

We proposed the optimization algorithm for liquid phase sintering of titanium alloy powder as shown in Figure 2.

TITANIUM ALLOY SIMULATION

The thermodynamic equilibrium calculations were performed using the software Thermo-Calc, Version R (Thermo-Calc Software, Stockholm, Sweden). Figure 3 shows the calculated Ti-Fe-Zr ternary phase diagram at the sintering temperature of 1,275°C. A liquid phase exists with solid phases that include bcc titanium, Laves phases, FeTi, and $Fe_{23}Zr_6$. In the present study, the compositions are adjusted to the

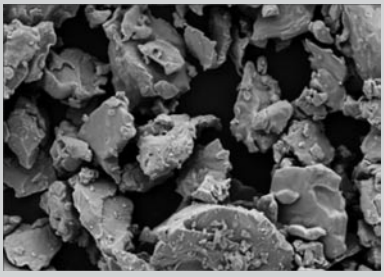

a

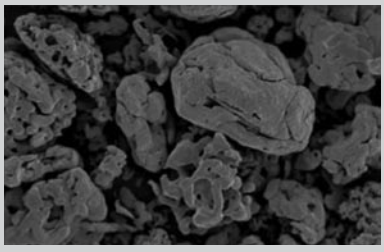

b

Figure 4. Scanning electron microscopy images for two titanium powders used in this research; (a) HDH titanium powder and (b) sponge titanium powder.

Table I. Equilibrium Phase Distribution for Different Ti Alloy Compositions at the Sintering Temperature of 1,275°C (wt.%)

No.	Ti	Fe	Mo	Zr	Sn	Cr	Mn	Cr_2C_3	bcc	fcc
Alloy 1	94.0	1	1	2	1	1	—	—	100	—
	88.0	2	2	4	2.5	1.5	—	—	100	—
	82.0	3	3	6	4	2	—	—	100	—
Alloy 2	93.0	1	1	2	1	1	1	—	100	—
	86.0	2	2	4	2.5	1.5	2	—	100	—
	79.0	3	3	6	4	2	3	—	100	—
Alloy 3	92.0	1	1	2	1	—	1	1	98.7	1.3
	83.0	2	2	4	2.5	—	2	3	93.9	6.1
	74.0	3	3	6	4	—	3	5	89.5	10.5

Table II. Characteristics of Raw Powders

Powder	Mesh Size	Purity	Powder Shape	Vendor
Ti (HDH)	–325	Commercial purity (CP)	Irregular	Phelly Mater.
Ti (sponge)	–100	Commercial purity (CP)	Round with pore	DuPont
Fe	–325	99.8	Irregular	Atlantic Eqp. Eng.
Zr	–325	99.9	Irregular	Alfa Aesar
Sn	–325	99.9	Irregular	Atlantic Eqp. Eng.
Mn	–325	99.6	Irregular	Atlantic Eqp. Eng.
Mo	–325	99.8	Irregular	Atlantic Eqp. Eng.
Cr	–325	99.8	Irregular	Atlantic Eqp. Eng.
Cr_2C_3	–325	99.8	Irregular	Atlantic Eqp. Eng.

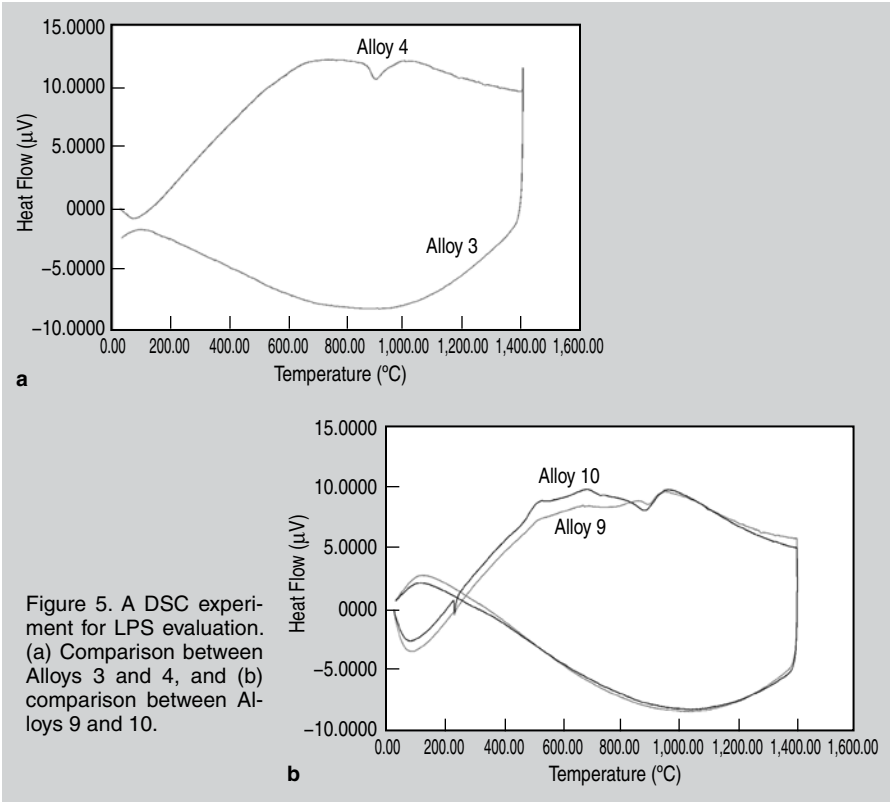

Figure 5. A DSC experiment for LPS evaluation. (a) Comparison between Alloys 3 and 4, and (b) comparison between Alloys 9 and 10.

range from 0 to 10 wt.% iron and 0 to 5 wt.% zirconium, where only bcc phase is obtained in the ternary system at the sintering temperature of 1,275°C.

The equilibrium phase calculations are performed at the sintering temperature of 1,523 K for the compositions suggested in the previous section. For each case, three values are chosen for each composition, which is low, middle, and high values of the selected compositions. The mass percentage of each phase is calculated for each composition, as shown in Table I. It can be seen that the bcc phase is dominant at the sintering temperature, while the fcc phase may appear if carbon is added. It is noted that no liquid phase is obtained for these compositions.

EXPERIMENTAL PROCEDURES

Preliminary Experiment

The two titanium powers used are shown in Figure 4: (a) hydride-dehydride (HDH; Phelly Materials) and (b) sponge (DuPont). To evaluate the alloys described in the previous section, additives included Fe, Mo, Zr, Sn, Mn, Cr, and Cr_2C_3. The characteristics of raw powders used in the experiment are listed in Table II.

We evaluated 15 titanium alloys as listed in Table II and selected six according to the following rank ordered criteria:

1. High sintered density from possible liquid phase sintering (LPS)
2. Clear endothermic peak for LPS
3. Cost of the alloy

To observe the endothermic peak for LPS, differential scanning calorimetry or DSC (SetSys Setaram Instrumentation Technologies) experiments were conducted over the temperature range of 25°C to 400°C with a constant heating rate of 10°C/min. An alumina crucible with a capacity of 75 μL was used for the mixed HDH titanium powder with the amount of additives as shown in Table II. Baseline correction was performed in two stages. First, a DSC run with empty crucible was subtracted from the experiment. Second, the data were corrected by assuming the combined effect of heat capacity differences and baseline fluctuations results in a heat flow, which is a second order polynomial**.** We used argon to investigate the effect of atmosphere. Figure 5 shows the DSC results. Alloy 10 shows more of an endothermic peak than Alloy 9 while Alloys 3 and 4 show no difference. We selected Alloy 9 obviously and Alloy 3 due to Criterion 3. Based on the above criteria, we selected six compositions as marked in Table III.

Based on the selected six titanium alloys, we proposed 16 new compositions with more combinations of the key additive elements, as listed in Table III. The amount of additives, as listed in Table III, was adjusted blended with HDH titanium powder for 30 min. The mixed powders were uniaxially compacted to a relative density 70% of theoretical at 600 MPa in a floating die to produce flat tensile bars. The sintering cycle was as follows: heat to 500°C at 10°C/min, hold for 60 min., heating at 10°C/min. to 1,275°C with 60 min. sintering in a vacuum below about 1 Pa (10 mtorr).

We measured sinter density and hardness for all alloys, as reported in Table III. The densities of the sintered samples were measured by means of the Archi-

Table III. Ti Alloys Evaluated and Selected*

Alloy ID		Ti	Fe	Mo	Zr	Sn	Mn	Cr	Cr_2C^3
1		97.0	1.5	1.5	—	—	—	—	—
2		94.0	3.0	3.0	—	—	—	—	—
3	Selected	94.5	1.5	1.5	2.5	—	—	—	—
4		89.0	3.0	3.0	5.0	—	—	—	—
5	Selected	93.0	1.5	1.5	2.5	1.5	—	—	—
6		86.0	3.0	3.0	5.0	3.0	—	—	—
7		91.5	1.5	1.5	2.5	1.5	1.5	—	—
8	Selected	83.0	3.0	3.0	5.0	3.0	3.0	—	—
9		90.5	1.5	1.5	2.5	1.5	1.5	1.0	—
10	Selected	81.0	3.0	3.0	5.0	3.0	3.0	2.0	—
11	Selected	89.5	1.5	1.5	2.5	1.5	1.5	1.0	1.0
12		79.0	3.0	3.0	5.0	3.0	3.0	2.0	2.0
13	Selected	83.0	3.0	3.0	6.0	4.0	—	1.0	—
14		81.0	3.0	2.0	6.0	4.0	3.0	1.0	—
15		76.0	3.0	3.0	6.0	4.0	3.0	—	5.0

* all amounts are in wt.%

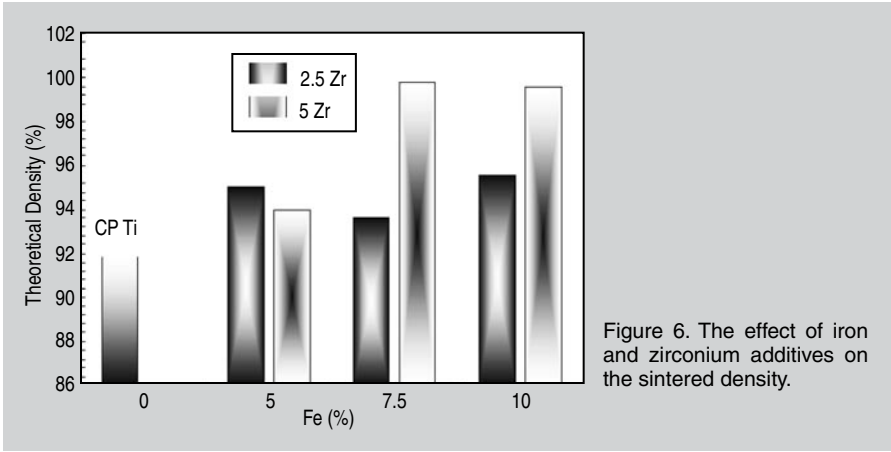

Figure 6. The effect of iron and zirconium additives on the sintered density.

medes water-immersion method. For metallographic examination, samples were cut from the center of the each sintered tensile test bar. The hardness tests were performed using a Leco-LR at HRB scale. At least five specimens were tested under the same conditions to ensure the reliability of the results. Based on the density measurement, we selected six compositions with the final sinter density higher than 94%, as shaded in Table IV.

For six selected alloys, we measured ultimate tensile strength (UTS) and elongation through tensile test, as reported in Table IV. All tensile tests were performed using an Instron-5569 mechanical tester at a constant crosshead speed of 1 mm/min. (25 mm gauge length). Note that two compositions, Ti-10Fe-2.5Zr-1.5Mo and Ti-10Fe-2.5Zr-4Cr_2C_3, proved to be too brittle for valid test results. Finally we selected Ti-xFe-yZr combinations as a candidate titanium alloy.

Experiments for Ti-Fe-Zr Alloys

The amount of additives was adjusted to give 0–10 wt.% iron and 0–5 wt.% zirconium and blended for 30 min. The mixed powders were uniaxially compacted to a relative density 70% of theoretical at 600 MPa in a floating die to produce flat tensile bars. The sintering cycle was as follows: heat to 500°C at a 10°C/min., hold for 60 min., heating at 10°C/min. to 1,275°C with 60 min. sintering in a vacuum below about 1 Pa (10 mtorr). Note that we used HDH titanium and sponge titanium powders in this experiment and the results are almost the same.

A set of sintering experiments was conducted at 1,275°C for 60 min. to study the effect of iron and zirconium addition on the theoretical density and the results are shown in Figure 6. As expected, CP titanium samples without iron and zirconium addition resulted in a maximum theoretical density of only 91.8%. At lower iron and zirconium levels such as 5% and 2.5 %, sintered density increases. When samples were admixed with 10% iron and 5% zirconium, a theoretical density of 99.6% was achieved. The iron and zirconium assisted sintering by the formation of a liquid phase produced by the eutectic reaction at 980–1,065°C. Favorable diffusion and solubility change promote densification in the presence of liquid phase. The liquid phase remains as an almost continuous network between solid grains, favoring the classical phenomenon of the liquid phase sintering. If the amount of iron, zirconium and the sintering temperature are correctly chosen, then near full density may be obtained.[6]

To observe the microstructure of the sintered titanium alloys, Kroll's reagent (3 mL HF, 6 mL HNO_3 in 100 mL H_2O) was used to etch the samples for optical metallography. The cross sections of

Table IV. Mechanical Properties for Selected Ti Alloys

		Green Sample		Sintered Sample (1,275°C, 60 min., 10 mtorr)				
Alloy	Theoretical Density (g/cm³)	Density (g/cm³)	Relative Density (%)	Density (g/cm³)	Relative Density (%)	Hardness (HRB)	Elongation (%)	UTS (MPa)
Pure Ti	4.51	3.24	71.8	4.14	91.8	88.1	3.13	643
Ti-5Fe-2.5Zr	4.64	3.26	70.2	4.41	94.9	103.9	3.54	1025
Ti-5Fe-5Zr	4.68	3.29	70.3	4.40	94.0	104.3	2.50	1227
Ti-10Fe-2.5Zr	4.75	3.21	67.6	4.54	95.6	108.1	0.60	611
Ti-10Fe-5Zr	4.79	3.43	71.6	4.77	99.6	112.9	0.00	281
Ti-5Fe	4.61	3.39	73.6	4.30	93.3	101.7	—	—
Ti-10Fe	4.71	3.26	69.2	4.40	93.4	104.5	—	—
Ti-10Fe-2.5Zr-1Cr	4.77	3.21	67.3	4.37	91.7	102.6	—	—
Ti-10Fe-5Zr-1Cr	4.81	3.34	69.5	4.43	92.2	104.4	—	—
Ti-10Fe-2.5Zr-1.5Mo	4.79	3.44	71.8	4.59	95.8	104.8	—	—
Ti-10Fe-2.5Zr-3Mo	4.83	3.41	70.5	4.45	92.0	105.4	—	—
Ti-10Fe-2.5Zr-2Sn	4.79	3.31	69.1	4.44	92.7	104.1	—	—
Ti-10Fe-2.5Zr-4Sn	4.83	3.55	73.5	4.46	92.4	103.4	—	—
Ti-10Fe-2.5Zr-2Cr_2C_3	4.78	3.16	66.1	4.38	91.6	105.2	—	—
Ti-10Fe-2.5Zr-4Cr_2C_3	4.81	3.28	68.1	4.53	94.1	108.3	1.40	373
Ti-10Fe-2.5Zr-1.5Mn	4.78	3.19	66.7	4.32	90.4	101.4	—	—
Ti-10Fe-2.5Zr-3Mn	4.81	3.19	66.3	4.37	90.9	103.7	—	—

sintered samples were examined using a scanning electron microscope (SEM; Zeiss).

Figure 7 shows the microstructures of the samples with and without iron and zirconium at different magnifications. The additive-free samples exhibit the porosity characteristic of low theoretical density as shown Figure 7a. Figure 7b and c shows the microstructures of the 5Fe-5Zr and 10Fe-5Zr samples, respectively. With 5Fe-5Zr addition, the amount of eutectic liquid is not sufficient for full densification and sintered density is 96% theoretical. On the other hand, 10Fe-5Zr addition samples exhibit enough eutectic phases at the grain boundaries. As a result, theoretical density increases with increasing amounts of liquid phase.

Figure 8 shows SEM images of Ti5Fe5Zr samples in different magnifications. According to these images, there is more porosity in the microstructure. On the contrary, theoretical density is very high. Results of SEM and EDX analysis show that the microstructure has embedded titanium grains within the matrix. These embedded grains are surrounded by a nitrogen-rich phase (TiN). Observation on almost all embedded grains indicates the presence of a nitrogen-rich phase and decohesion with the matrix.

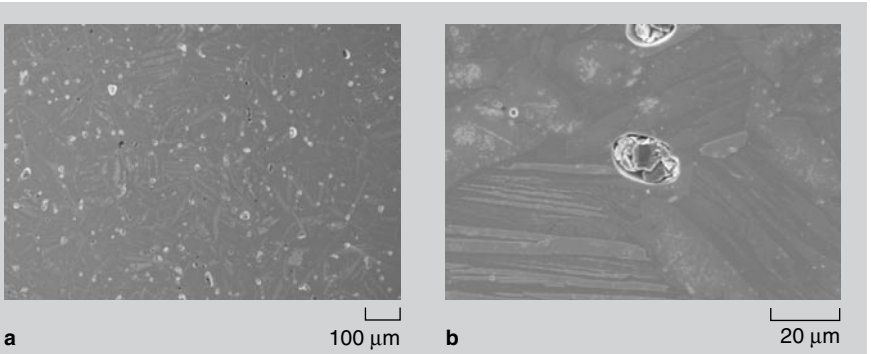

Figure 8. Scanning electron microscopy images of a Ti-5Fe-5Zr sintered sample at different magnifications.

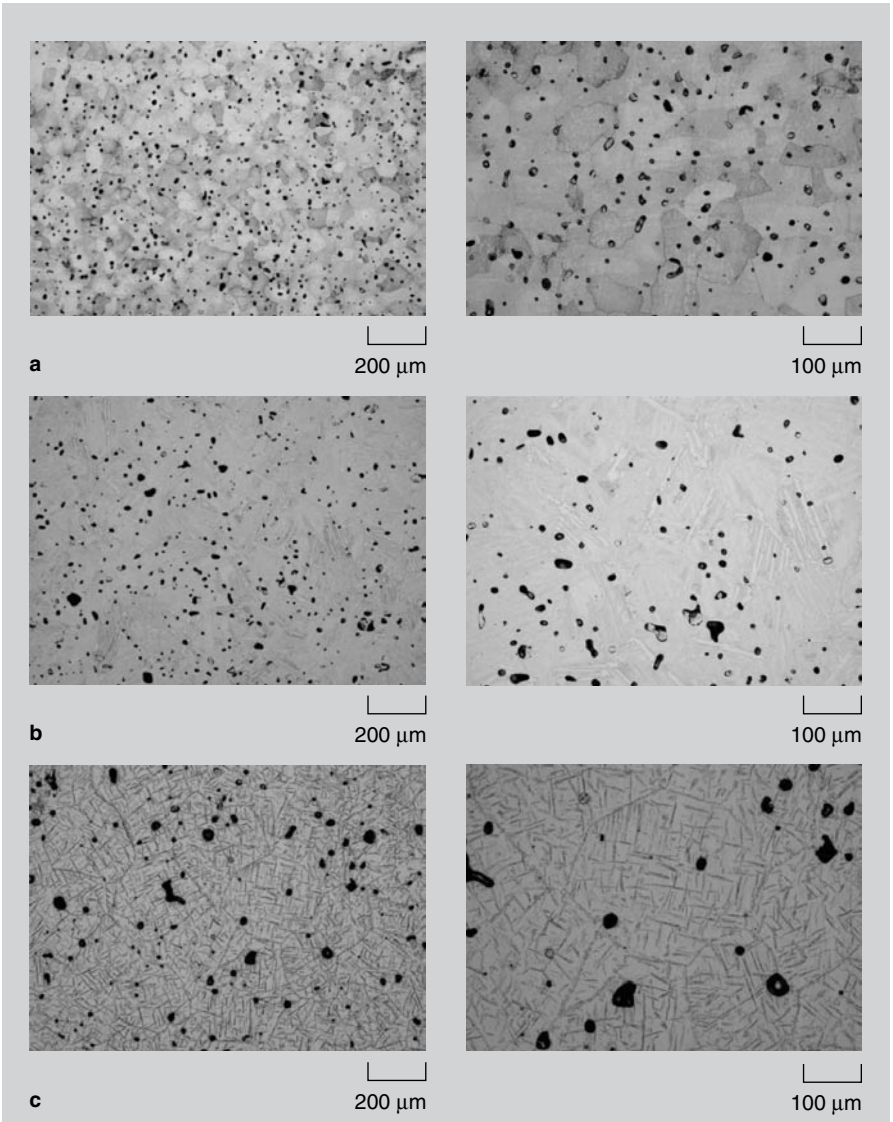

Figure 7. Optical micrographs of (a) CP Ti, (b) 90Ti–5Fe–5Zr, and (c) 85Ti–10Fe–5Zr samples.

The effect of iron and zirconium additions on the mechanical properties of Ti-Fe-Zr alloys is shown in Figure 9a, b, and c. Commercially pure titanium samples present average mechanical properties, especially elongation, similar to iron and zirconium added samples. The tensile strength was increased with the amount of alloying. Tensile strength decreased with iron additions at 7.5% and 10% iron, due to the presence of brittle intermetallic along the grain boundaries. Ductility decline is even more drastic with iron and zirconium addition samples. The maximum tensile strength and elongation of 1,227 MPa and 3.5% were measured for titanium with 5Fe and 5Zr additions. The effect of iron and zirconium additions on the hardness of Ti-Fe-Zr alloy is shown in Figure 9c. The results of hardness measurements exhibited an increasing trend similar to that of theoretical density. The highest hardness was obtained with the highest sintered density attained. A maximum hardness of 113 HRB was reached with 10Fe and 5Zr additions.

The morphologies of fracture surface of the CP Ti and Ti-Fe-Zr alloy samples after sintering at 1,275°C for 60 min. are shown in Figure 10. The fracture surface of CP Ti samples exhibit dimpled features and porosities as shown in Figure 10a. The morphology of features surface with 5% iron and 5% zirconium addition is shown in Figure 10b. This sample exhibits quasi-cleavage fracture and low porosity. The morphology of fracture with 10% iron and 5% zirconium addition is shown in Figure 10c. This sample exhibited a very brittle

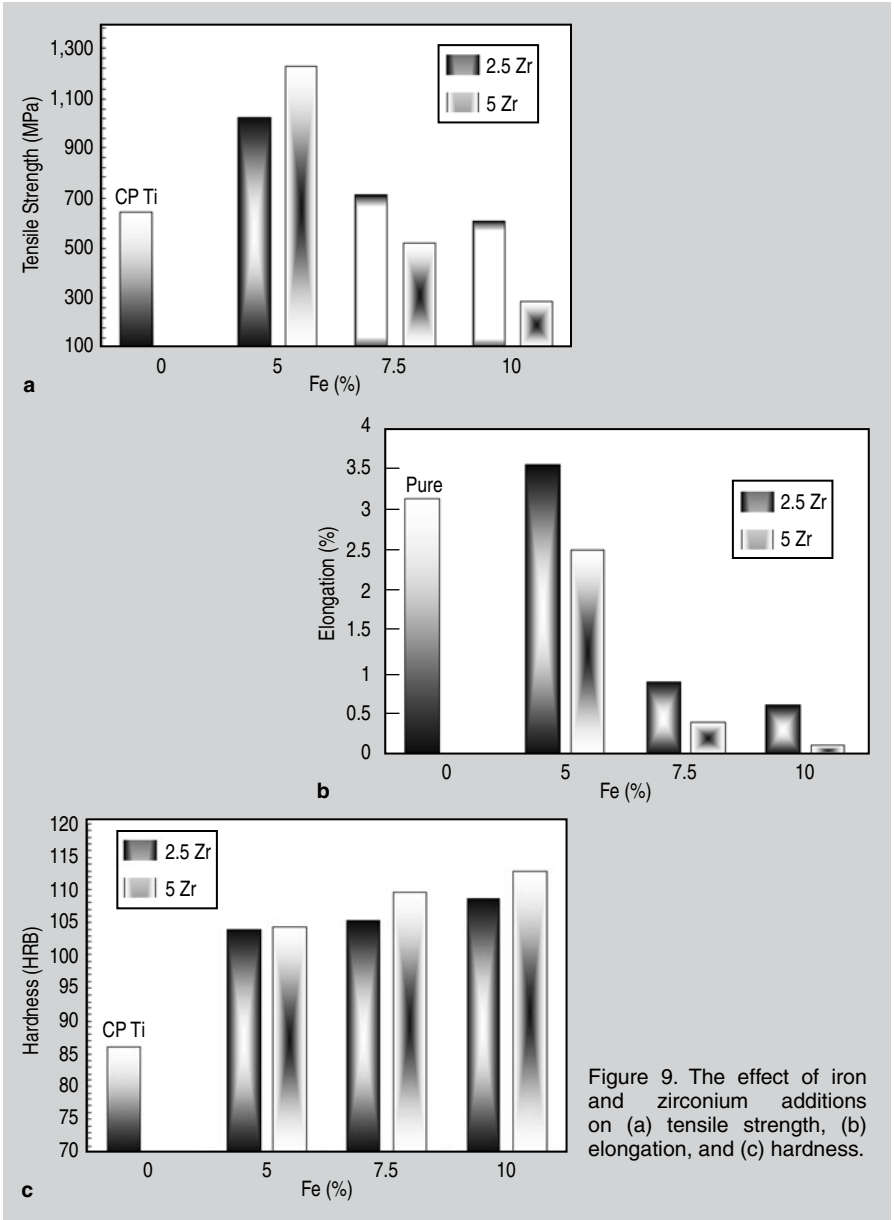

Figure 9. The effect of iron and zirconium additions on (a) tensile strength, (b) elongation, and (c) hardness.

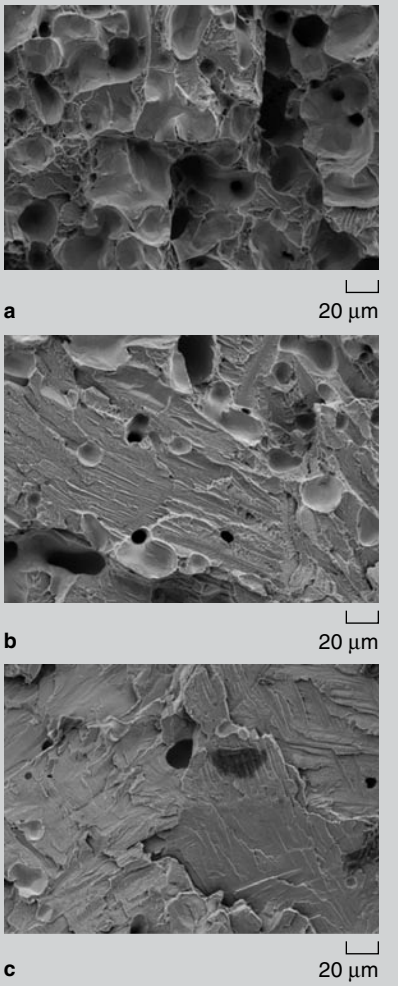

Figure 10. Fractographs of samples (a) CP Ti, (b) 90Ti-5Fe-5Zr, and (c) 85Ti-10Fe-5Zr.

fracture. In this case the brittle fracture occurred through the intermetallic liquid phase network. The eutectic network improved sintered density and mechanical properties and decreased porosity.

CONCLUSIONS

The addition of iron and zirconium to a CP Ti powder showed at concentrations of 5 wt.% iron and 5 wt.% zirconium there was a beneficial effect of the liquid phase sintering phenomenon. The alloying and densification with vacuum sintering at 1,275°C for 60 min. resulted in a tensile strength of 1,227 MPa and hardness of 104 HRB. These values correspond to an increase of 90% and 21%, respectively, as compared to CP Ti powder processed under the same conditions without the additives. The promotion of liquid phase sintering, a well-established option in PM, is a possible means to cost-effectively extend the use of titanium for a broader range of net-shape PM products.

References

1. C. Leyens and M. Peters, *Titanium and Titanium Alloys* (Weinheim, German: WILEY-VCH Verlag GmbH & Co. KGaA, 2003).
2. H. Fujii and K. Takahashi, "Development of High Performance Ti-Fe-Al Alloy Series," *Nippon Steel Technical Report*, 85 (2002), pp. 113–117.
3. S. Krishnamurthy et al., *Progress in Powder Metallurgy*, 39 (1984), pp. 603–623.
4. G. Adam et al., *Advanced Materials Research*, 29-30 (2007), pp. 147–152.
5. G. Lutjering and J. C. Williams, *Titanium*, 2nd Edition (Berlin, German: Springer, 2007).
6. R.R. Boyer, *Materials Science and Engineering A*, 213 (1996), pp. 103–114.
7. B. Liu, et al., *Transactions of Nonferrous Metals Society of China*, 18 (2) (2008), pp. 227–232.
8. F. Sun and O. Yu, *Innovations in Titanium Technology,* ed. M.N. Gungor, M.A. Imam, and F.H. Froes (Warrendale, PA: TMS, 2007), pp. 19–27.
9. V. Moxson et al., *International Journal of Powder Metallurgy*, 34 (5) (1998), pp. 127–134.
10. W. Wei et al., *Powder Metall.*, 46 (3) (2003), pp. 246–250.
11. Y. Liu et al., *Materials Science & Engineering A*, A418 (2006), pp. 25–35.
12. D. Kuroda et al., *Mater. Sci. Eng. C*, 25 (2005), pp. 312–320.
13. T. Fujita et al., *Materials Science & Engineering A*, A213 (1-2) (1996), pp. 148–153.
14. V.A. Duz et al., *Cost-Affordable Titanium,* ed. F.H. Froes, M.A. Imam, and D. Fray (Warrendale, PA: TMS, 2004), pp. 145–150.
15. X. Zhang et al., *Scripta Mater.,* 41 (1999), pp. 39–46.
16. E. Yun, K. Lee, and S. Lee, *Surf. Coat. Technol.*, 184 (2004), pp. 74–83.
17. R. Banerjee et al., *Scripta Mater.*, 53 (2005), pp. 1433–1437.
18. F. Wang, J. Mei, and X. Wu, *Journal of Materials Processing Technology*, 195 (1-3) (2008), pp. 321–326.

Haitham El Kadiri, Liang Wang, Seong Jin Park, and Youssef Hammi are with the Center for Advanced Vehicular Systems, Mississippi State University, 200 Research Blvd., Starkville, MS 39759, USA; H. Ozkan Gulsoy is with Marmara University, Material Department, Istanbul, Turkey; Pavan Suri is with Heraeus Inc., Chandler, Arizona; and Randall M. German is with the College of Engineering, San Diego State University, San Diego, California. Dr. Park can be reached at sjpark@cavs.msstate.edu.